Agricultural and Forest Meteorology 276–277 (2019) 107651

Contents lists available at ScienceDirect

Agricultural and Forest Meteorology

journal homepage: www.elsevier.com/locate/agrformet

Evaluating a Lagrangian inverse model for inferring isotope CO_2 exchange in plant canopies

Marshall Santos[a], Eduardo Santos[b,*], Claudia Wagner-Riddle[c], Shannon Brown[c], Kyle Stropes[b], Ralf Staebler[d], Jesse Nippert[b]

[a] Federal University of Viçosa, Brazil
[b] Kansas State University, United States
[c] University of Guelph, Canada
[d] Environment and Climate Change Canada

ARTICLE INFO

Keywords:
Isotope flux ratio method
Lagrangian dispersion analysis
Localized near-field theory
Plant canopies
Stable isotopes of CO_2
Tunable diode laser spectroscopy

ABSTRACT

Multi-layer Lagrangian models could be useful techniques for studying stable isotope exchange within and just above plant canopies. The main objective of this study was to evaluate the use of an analytical Lagrangian analysis (localized near-field theory, LNF), to study $^{13}CO_2$ and $C^{18}OO$ isotope exchange in different plant canopies by comparing the LNF estimates with those provided by the eddy covariance (EC) technique and the isotope flux ratio method (IFR). Mixing ratios of stable isotopes of CO_2 were measured within and above a temperate deciduous forest, tallgrass prairie and corn field using a multi-port sampling system and the tunable diode laser spectroscopy technique. Wind velocity data and the net CO_2 ecosystem exchange (NEE) were measured above the plant canopies using an EC system. The wind velocity data and CO_2 stable isotope mixing ratios were combined with the LNF theory to infer NEE and source/sinks of isotopes inside canopies. The LNF NEE estimates were likely affected by the flux decoupling in the forest canopy, resulting in a low correlation (R^2 ranging from 0.03 to 0.35) between LNF and EC NEE estimates. On the other hand, LNF NEE estimates for corn and grassland canopies showed better correlation with EC NEE estimates (R^2 ranging from 0.58 to 0.85), suggesting better coupling between in and above canopy air flows. Although, both LNF and IFR estimates showed large variability, our results show that the LNF approach reduced the uncertainties of the isotope compositions of NEE when compared to the IFR approach. These results suggest that LNF is a useful tool to study CO_2 isotope exchange within short canopies where flux measurements are more challenging than inside tall canopies.

1. Introduction

Stable isotopes of carbon dioxide and water vapour are useful tools to investigate biophysical processes in ecosystems (Griffis, 2013; Werner et al., 2012). High temporal resolution and accurate isotope measurements suitable for ecosystem scale studies have become available with recent advancements in laser spectroscopy techniques. These advancements allowed the development of field-deployable trace gas analysers capable of providing accurate and near-continuous isotope measurements under field conditions (Griffis, 2013). Recently, atmospheric concentrations of CO_2 and H_2O isotopologues started to be monitored continuously at different ecosystems across the United States (SanClements et al., 2014). These concentration measurements can bring new insights into the biophysical mechanisms governing the isotope exchange in ecosystems as they provide a transient imprint of isotope sources and sinks in the biosphere (Raupach, 2001).

Micrometeorological approaches, such as the eddy covariance technique (Griffis et al., 2011; Sturm et al., 2012; Wehr et al., 2013; Wehr and Saleska, 2015) and the flux gradient approach (Griffis et al., 2005b, 2004; Santos et al., 2012; Yakir and Sternberg, 2000) have been used to study isotope exchange in ecosystems. The eddy covariance (EC) approach is a well-stablished micrometeorological method widely used to measure CO_2 and energy fluxes in several sites around the world (Baldocchi, 2003; Xiao et al., 2012). Griffis et al. (2008) applied the EC technique to measure CO_2 isotope exchange above a soybean canopy. They found a relatively good agreement between the isofluxes measured using the EC method with the ones provided by the flux gradient method. However, the high cost of fast response sensors required for EC measurements constrains the widespread use of the EC technique to quantify stable isotope exchange in ecosystems.

The isotope flux ratio (IFR) method has been used as an alternative to

* Corresponding author.
E-mail address: esantos@ksu.edu (E. Santos).

https://doi.org/10.1016/j.agrformet.2019.107651
Received 31 January 2019; Received in revised form 27 June 2019; Accepted 29 June 2019
Available online 05 July 2019

measure isotope exchange in ecosystems (Griffis et al., 2005b, 2004; Santos et al., 2012). The IFR method is based on the gradient-diffusion theory (K-theory), which relates the mean turbulent vertical flux to mean concentration gradients measured above plant canopies (Denmead and Bradley, 1987; Griffis et al., 2004). When compared to the EC approach, a major advantage of the IFR method is that this approach does not require fast response gas analysers. In addition, flux gradient approaches allow multiple sites to be measured near-simultaneously with a single trace gas analyser combined with a multiport sampling system (Brown and Wagner-Riddle, 2017). However, the accuracy of the IFR estimates is quite sensitive to errors in measurements of concentration gradients. Small gradients of concentration often lead to large uncertainties in estimates of the isotope exchange due to the small signal to noise ratio of concentration gradients (Griffis, 2013; Griffis et al., 2005a). One alternative to increase the signal to noise ratio of concentration gradient measurements is to take concentration measurements inside plant canopies where vertical gradients of concentration are often strong (Buchmann et al., 1996). However, flux-gradient methods are prone to errors within the canopies due the proximity of source/sinks of scalars as well as to the presence of turbulent eddies with length scales larger than the distance over which vertical gradients of concentration are measured (Corrsin, 1975; Denmead and Bradley, 1987; Raupach, 1987).

Multi-layer Eulerian and Lagrangian models have been applied to study the dispersion of scalars within plant canopies (Katul et al., 1997; Katul and Albertson, 1999; Raupach, 1989a, 1989b; Siqueira et al., 2000; Warland and Thurtell, 2000). The Lagrangian dispersion models infer the average scalar concentration field by tracking the position of small fluid particles (Raupach, 2001). This leads to a better description of the turbulent motions responsible for the dispersion of scalars within plant canopies in comparison to the flux-gradient theory (Raupach, 1987; Warland and Thurtell, 2000). Lagrangian dispersion models can be used to solve the so-called forward problem, i.e. to determine a scalar concentration field from scalar source/sink distributions (S). But for most practical applications these models are used to solve the inverse problem, in which S is inferred based on turbulent statistics and mean scalar concentration gradients measured above and inside plant canopies (Raupach, 1989a, 1989b).

The localized near-field (LNF) theory, proposed by Raupach (1989a), is a multi-layer Lagrangian canopy model that has been used for inferring scalar source/sink distributions and fluxes of heat, water vapour, CO_2 and other traces gases within different plant canopies (Harper et al., 2000; Katul et al., 1997; Katul and Albertson, 1999; Leuning et al., 2000; Raupach et al., 1992; Siqueira et al., 2000; Ueyama et al., 2014). Currently, studies applying multi-layer Lagrangian models to quantify isotope exchange in plant canopies are scarce (Haverd et al., 2011; Santos et al., 2012; Styles et al., 2002). Styles et al. (2002) applied a canopy scale model, based on the LNF theory, combined with a sun and shade photosynthesis and energy balance model, to infer scalar source/sink distributions, including for $^{13}CO_2$, in a Siberian mixed-coniferous forest. Their results showed great deviation between modelled and measured $\delta^{13}C$ profiles, which was attributed to instrument precision limitations, and insufficient isotope sampling rate that did not capture rapid isotope concentration changes mainly at sunrise and sunset. Haverd et al. (2011) used the LNF theory combined with source/sink distributions of deuterium (HDO) composition of water vapour, estimated using an isotopically enabled soil vegetation atmospheric transfer model, for partitioning the evapotranspiration into soil evaporation and transpiration in a forest canopy. Both of these studies were limited to sampling campaigns in forest canopies over a few weeks. A more complete evaluation of the potential in combining the LNF theory to study isotope exchange could be obtained using larger datasets for canopies with different heights and structures.

In the present study, we used several months of near-continuous measurements of stable isotopes of CO_2 collected in three different ecosystems to quantify canopy level isotope exchange. The main objective of this study was to evaluate the performance of the LNF theory to estimate isotope exchange in plant canopies by comparing its estimates with values provided by the IFR method.

2. Material and methods

2.1. The localized near-field theory

The concentration field near plant canopies can be regarded as the result of contributions of different instantaneous sources inside the canopy. The LNF theory is a semi-Lagrangian dispersion analysis that divides the concentration field into near-field (C_n) and far-field (C_f) regions (Raupach, 1989a, 1989b). In the near-field region, the fluid particle dispersion is governed by the persistence of the Lagrangian velocity relative to the scalar source, while in the far-field region random motions of fluid particles dominate the scalar transport (Taylor, 1922). The LNF theory centres on the evaluation of a transition probability function, which is divided into far-field and near-field terms, and provides statistical means of determining the marked-fluid particle position distributions (Raupach, 2001).

The discrete form of the LNF theory assumes that for a horizontally homogeneous plant canopy and steady turbulent conditions, the scalar source densities and concentrations are only a function of height (z). In addition, the scalar concentration at a given level inside the canopy is assumed to be the result of near-field and far-field contributions from m horizontally homogenous source/sink layers with thickness Δz_j located inside the canopy. The mean scalar concentration (c_i) can be related to the source/sink strength through a dispersion matrix (Raupach, 2001), as follows:

$$c_i - c_R = \sum_{j=1}^{m} \boldsymbol{D}_{ij} S_j \Delta z_j \tag{1}$$

where i and j are indices corresponding to concentration (c) and source (S) layers, respectively, c_R is the scalar concentration at a reference level (z_R), and $\mathbf{D}_{ij}$ is the dispersion matrix. The dispersion matrix ($\mathbf{D}_{ij}$) is essentially a discrete form of a particle distribution transition probability function and provides a prediction of the position of the fluid particles within and above the canopy over time. For the calculation of $\mathbf{D}_{ij}$ terms, $\mathbf{D}_{ij}$ is divided into far field ($\mathbf{D}_{ij}^{(F)}$) and near field ($\mathbf{D}_{ij}^{(N)}$) parts:

$$\mathbf{D}_{ij} = \mathbf{D}_{ij}^{(F)} + \mathbf{D}_{ij}^{(N)} \tag{2}$$

The elements of $\mathbf{D}_{ij}^{(F)}$ are given by:

$$\mathbf{D}_{ij}^{(F)} = \int_{\max(z_i,\ Z_j)}^{z_R} \frac{dz'}{\sigma_w^2(z')\,T_L(z')} \tag{3}$$

where z_i is the concentration measurement heights, Z_j is the height in the center of the source layer, σ_w is the standard deviation of the wind vertical velocity and T_L is the Lagrangian time scale.

The near-field part of $\mathbf{D}_{ij}$ is given by

$$\mathbf{D}_{ij}^{(N)} = \frac{1}{\sigma_{wj}}\left[k_N\left(\frac{z_i - Z_j}{\sigma_{wj}\,T_{Lj}}\right) + k_N\left(\frac{z_i + Z_j}{\sigma_{wj}\,T_{Lj}}\right) - k_N\left(\frac{z_r - Z_j}{\sigma_{wj}\,T_{Lj}}\right) - k_N\left(\frac{z_r + Z_j}{\sigma_{wj}\,T_{Lj}}\right)\right] \tag{4}$$

for z_i not in (z_{j-1}, z_j)

$$\mathbf{D}_{ij}^{(N)} = \frac{T_{Lj}}{\Delta z_j}\left[I_N\left(\frac{z_i - z_{j-1}}{\sigma_{wj}\,T_{Lj}}\right) + I_N\left(\frac{z_j - z_i}{\sigma_{wj}\,T_{Lj}}\right)\right] + \frac{1}{\sigma_{wj}}\left[k_N\left(\frac{z_i + Z_j}{\sigma_{wj}\,T_{Lj}}\right) - k_N\left(\frac{z_r - Z_j}{\sigma_{wj}\,T_{Lj}}\right) - k_N\left(\frac{z_r + Z_j}{\sigma_{wj}\,T_{Lj}}\right)\right] \tag{5}$$

for z_i in (z_{j-1}, z_j)

where k_N (ζ) is the "near-field kernel" which represents the near-field contribution for a unit plane source at z_0, and I_N (ζ) is defined as the integral of k_N (ζ) from 0 to ζ. The adimensional variable ζ represents the height interval z - z_0 (Raupach, 1989c). Further details about the calculation of the far-field and near-field parts of $\mathbf{D}_{ij}$ can be found in

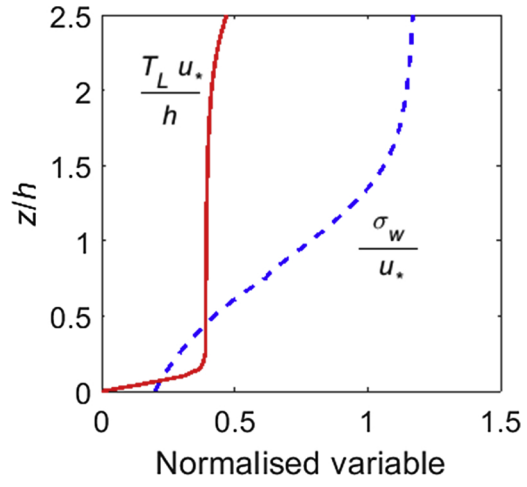

Fig. 1. Normalized profiles of Lagrangian time scale (T_L, red solid line) and standard deviation of vertical wind velocity (σ_w, blue dashed line) calculated using the turbulence statistics parameterization proposed by Leuning (2000). The symbols z, u_* and h denote: above ground height, friction velocity and canopy height, respectively. (For interpretation of the references to colour in this figure legend, the reader is referred to the web version of this article).

Raupach (2001).

In this study, profiles of T_L and σ_w were estimated using parameterization of turbulence statistics proposed by Leuning (2000) (Fig. 1). The generated turbulent statistics profiles (σ_w and T_L) were corrected for atmospheric stability conditions as suggested by Leuning (2000).

To infer source strength using scalar concentration measurements, the dispersion matrix ($\mathbf{D}_{ij}$) is computed by dividing the canopy into m source layers (S_j). Measurement errors in concentration profiles can introduce uncertainties in the LNF results. Raupach (2001) recommended the use of redundant concentration data to minimize these uncertainties, by ensuring that m is smaller than n.

The scalar source strength is obtained from Eq. (1), by solving a system of m linear equations (Raupach, 1989a):

$$\sum_{k=1}^{m} A_{jk} S_k = B_j \text{ with} \begin{cases} A_{jk} = \sum_{i=1}^{n} \boldsymbol{D}_{ij} \Delta z_j \boldsymbol{D}_{ik} \Delta z_k \\ B_j = \sum_{i=1}^{n} (c_i - c_R)_{(\text{means})} \boldsymbol{D}_{ij} \Delta z_j \end{cases} \quad (6)$$

The scalar flux for each source layer (F_j) is given by:

$$F_j = \sum_{j=1}^{m} S_j \Delta z_j \quad (7)$$

The net flux (F_N) is obtained by adding F_j values for all source layers. The estimated F_N for lighter and heavier isotopes were converted to delta notation (δ_N, ‰) as follows:

$$\delta_N = \frac{R_N}{R_{VPDB}} - 1 \quad (8)$$

where R_N is the ratio of the heavier to lighter isotopologues fluxes (F_N^H / F_N^L) defined as F_N^H / F_N^L for $^{13}CO_2$ and $^{12}CO_2$ fluxes, or 0.5 F_N^{18} / F_N^{16} for $C^{18}O^{16}O$ and $C^{16}O_2$ fluxes, and R_{VPDB} represents the standard molar ratio ($^{13}C/^{12}C$ or C^{18}/C^{16}) of the Vienna Pee Dee Belemnite.

2.2. The isotope flux ratio method

The isotope flux ratio (IFR) method proposed by Griffis et al. (2004) is based on the flux-gradient theory, which assumes that: (1) the turbulent transfer in the inertial sublayer above plant canopies is analogous to molecular diffusion, and (2) the turbulent flux is proportional to the product of the mean vertical concentration gradient and the eddy diffusivity (Corrsin, 1975). The IFR method allows calculating the ratio between fluxes of heavier and lighter isotopologues, as follows:

$$\frac{F_N^H}{F_N^L} = \frac{-(K\,\overline{\rho_a}/M_a)\mathrm{d}[\bar{H}]/\mathrm{d}z}{-(K\,\overline{\rho_a}/M_a)\mathrm{d}[\bar{L}]/\mathrm{d}z} \quad (9)$$

where K is the eddy diffusivity, which is assumed to be the same for heavy and light isotopologues, $\overline{\rho_a}$ is the mean density of dry air, M_a is the molar mass of dry air, and $\mathrm{d}[\bar{L}]/\mathrm{d}z$ and $\mathrm{d}[\bar{H}]/\mathrm{d}z$ are the time-averaged vertical gradients of the heavy and light isotopologues. After some simplifications, Eq. (9) can be rewritten in a discrete form as follows:

$$\frac{F_N^H}{F_N^L} = \frac{[\bar{H}]_{z_2} - [\bar{H}]_{z_1}}{[\bar{L}]_{z_2} - [\bar{L}]_{z_1}} \quad (10)$$

where $[\bar{H}]$ and $[\bar{L}]$ are the half-hourly mean mixing ratios of isotopologues at two heights (z_1 and z_2) above the canopy.

Lastly, the ratio of isotopologues fluxes (F_N^H / F_N^L) were converted to delta notation using Eq. (8). Thus, the isotope composition of F_N (δ_N) provided by the IFR method was directly compared with the LNF estimates.

2.3. Experimental sites

Field experiments were carried out at three sites: 1) the Borden Forest Research Station; 2) the Konza Prairie Biological Station; and 3) the Elora Research Station. The site locations, vegetation types and measurement periods are summarized in Table 1. Further experimental details about the sites is given by Santos et al. (2012), (2011) and Stropes (2017).

2.4. Isotope measurements

The mixing ratios of the CO_2 isotopologues ($^{12}C^{16}O_2$, $^{13}CO_2$ and $C^{18}OO$ for the forest; $^{12}C^{16}O_2$ and $^{13}CO_2$ for grassland and corn) were measured at a frequency of 10 Hz using tunable diode laser trace gas analysers (TGA100A or TGA200, Campbell Sci., Logan, UT, USA). Table 2 provides information of isotope measurements for each site. The ambient air was sampled using eight air intakes, set up within and above the canopies. Each air intake consisted of a 1 m-long stainless tube (0.43 cm I.D.) with a rain diverter. Inline-stainless filters (SS-4F-K4-7, 7 µm sintered element filter, Swagelok, OH, USA) were positioned downstream from each air intake. To prevent water vapour condensation inside the filters and sampling lines, the filter holder was heated using a 0.5 W heater connected to a 12 V DC power supply, and a critical flow orifice located downstream of the filter was used to reduce the air pressure in the sampling line. The sampling lines were directed

Table 1
Location, vegetation type and measurement periods at the three experimental sites: Borden Forest Research Station (BFRS), Konza Prairie Biological Station (KPBS) and Elora Research Station (ERS).

Site	Location	Vegetation	Measurement period
BFRS	Borden, ON, Canada (44º 19'N, 79º 56'W)	mixed deciduous forest	August to September, 2009
KPBS	Manhattan, KS, USA (39° 59'N, 96°34'W)	native tallgrass prairie	September to November, 2015
ERS	Elora, ON, Canada (43º 39'N, 80º25'W)	corn (*Zea mays* L.)	August to October, 2008

Table 2
Isotope measurement instrumentation, measured isotopologues, canopy and air intake heights at the three experimental sites. Refer to Table 1 for the meaning of the site acronyms.

Site	Gas analyzer	Measured isotopologues	Canopy height (m)	Air intake heights (m)
BFRS	TGA100A	$^{12}C^{16}O_2$, $^{13}CO_2$ and $C^{18}OO$	22.0	0.45, 1.45, 5.51, 9.65, 16.69, 20.77, 25.81 and 36.81
KPBS	TGA200	$^{12}C^{16}O_2$ and $^{13}CO_2$	1.3	0.18, 0.31, 0.45, 0.56, 0.73, 1.29, 2.00 and 3.00
ERS	TGA100A	$^{12}C^{16}O_2$ and $^{13}CO_2$	2.4	0.16, 0.63, 1.03, 1.47, 1.86, 2.25, 2.75 and 3.15

to a custom-made manifold (Campbell Scientific, Logan, UT) that controlled the flow of ambient air from the air inlets and calibration gases through the TGA. The air was drawn continuously through all air intakes at a flow rate of approximately 600 mL min^{-1} using a vacuum pumps. A sub-sample of the total flow was directed to the TGA with a flow rate of approximately 200 mL min^{-1}. The manifold also kept the TGA sample cells at constant operating pressures (TGA100A at 1.8 kPa and TGA200 at 3 kPa). Each air intake was measured for 15 s at BFRS and ERS sites and for 30 s at KPBS. The longer intake sampling time at KPBS took into account the longer residence time of the air within the TGA200 sampling cell.

2.5. Flux measurements

At all sites, the NEE was measured continuously above the canopies by EC systems. A sonic anemometer (CSAT3, Campbell Sci.) and open-path CO_2/H_2O infrared gas analyzer (LI-7500, LI-COR, Lincoln, NE, USA) were used to measure the three wind components and CO_2 mixing ratios, respectively. The EC system was installed at 33.4 m for the forest, 2.5 m for the grassland and 2.84 m for the corn canopy. All sensor signals were recorded at 20 Hz using dataloggers (CR3000 and CR23X, Campbell Sci.).

3. Results and discussion

3.1. CO_2 mixing ratio and isotope composition of the air

The CO_2 mixing ratios were usually higher near the ground than near the canopy top and during the nighttime periods at all sites (Fig. 2d–f) when compared to daytime values. The grassland site showed a smaller spatial variability in [CO_2] in comparison to the corn and forest canopies (Fig. 2b and e). The smaller [CO_2] gradients at the grassland site can be explained by the fact the measurements at this site were taken near the end of the growing season (Table 1), when [CO_2] gradients and fluxes were often smaller than the ones expected for the peak of the growing season. The average (± SD) NEE over the measurement period ranged from -8.5 ± 11.1 μmol m^{-2} s^{-1}, −1.1 ± 8.4 μmol m^{-2} s^{-1} and −0.4 ± 7.3 μmol m^{-2} s^{-1} for the corn, forest and grassland ecosystems, respectively. The forest and corn sites showed a distinct [CO_2] diel pattern, with the highest [CO_2] values being observed just before sunrise (4–6:00 h) and low [CO_2] during mid-day (Fig. 2a and c). The high [CO_2] in the early morning is a result of continuous build-up of respiratory CO_2 throughout the night when turbulent mixing is low (Buchmann et al., 1996). The diel [CO_2] variation is in agreement with previous studies and is a result of the changes in atmospheric boundary layer and turbulent mixing, as well as photosynthetic uptake and ecosystem respiration (Buchmann et al., 1996; Buchmann and Ehleringer, 1998; Hsieh et al., 2003).

The $^{13}CO_2$ (and $C^{18}OO$ for the forest) compositions of atmospheric air (δ_a^{13} and δ_a^{18}, respectively) were less negative during daytime than night-time (Fig. 3). These diel patterns of δ_a^{13} and δ_a^{18} are driven primarily by the isotope enrichment of the atmospheric air during daytime due to photosynthetic fractionation and changes in the atmospheric boundary layer (Farquhar et al., 1989). The opposite trend was observed during night-time, when ecosystem respiration releases CO_2 to the atmosphere depleted in heavy isotopologues ($^{13}CO_2$ and $C^{18}OO$) and atmospheric mixing is low (Flanagan et al., 1996; Yakir and Sternberg, 2000).

There was also a clear distinction between δ_a^{13} (and δ_a^{18} for forest) daytime and night-time profiles (Fig. 3b, d, f and h). For grassland (Fig. 3e and f) and corn (Fig. 3g and h) canopies, the δ_a^{13} gradients were smaller than the ones measured at the forest site, which could be in part explained by the lower discrimination against $^{13}CO_2$ by C_4 species (corn and grassland) in comparison to the forest vegetation. In addition, in taller forest canopies the large air volume and lower air mixing within the canopy contribute to large gradients of scalar concentration (Fig. 3b and d). Conversely, in short canopies such as grassland and corn, the air volume within the canopy is smaller which could promote better turbulent mixing in these short canopies.

3.2. LNF estimates of CO_2 source strength distributions and CO_2 fluxes

To investigate the performance of the LNF theory in estimating net scalar fluxes, the NEE computed by LNF was compared with the NEE measured using the EC technique. We also investigated the effect of different friction velocity (u_*) values on the relationship between LNF and EC estimates (Table 3). In general, the correlation and agreement, expressed respectively by the R^2 and refined index of agreement (d_r) (Willmott et al., 2012), for LNF and EC NEE relationships, improved as the u_* values increased (Table 3). However, for the grassland site, a slightly better correlation between EC and LNF NEE estimates were found for $u_* > 0.3$ m s^{-1} ($R^2 = 0.91$) than for $u_* > 0.4$ m s^{-1} ($R^2 = 0.88$), where very good agreements ($d_r = 0.99$) were found for both cases. Considering only the NEE data for $u_* > 0.4$ m s^{-1}, the grassland canopy showed the best correlation ($R^2 = 0.88$) and agreement ($d_r = 0.99$) between EC and LNF NEE estimates, followed by corn ($R^2 = 0.72$ and $d_r = 0.83$) and forest canopies ($R^2 = 0.35$ and $d_r = 0.96$). Although stricter u_* values tended to improve correlation and agreement between the methods, they also resulted in a drastic decrease in the number of NEE available data points (Table 3).

To evaluate the dependence of LNF on atmospheric stability, we separated the observed and modelled NEE in classes based on the atmospheric stability conditions (Table 4). The atmospheric stability condition was determined by the ratio between the canopy height and the Obukhov length (h/L), and classified as: unstable ($-0.01 < h/L$), neutral ($-0.01 \leq h/L < 0.01$) and stable ($h/L \geq 0.01$). Considering only the NEE data for $u_* > 0.1$ m s^{-1} (Table 4), the forest showed a very poor correlation between measured and modelled NEE under unstable conditions ($R^2 = 0.21$), and a reasonable to poor correlation under neutral ($R^2 = 0.43$) and stable conditions ($R^2 = 0.35$), respectively. For the grassland, higher correlation between measured and modelled NEE was found when the atmosphere was unstable ($R^2 = 0.87$), following by near neutral ($R^2 = 0.61$) and stable ($R^2 = 0.20$) conditions. For the corn canopy, a very poor correlation between measured and modelled NEE was found when the atmosphere was stable ($R^2 = 0.12$), however, higher correlation was observed under unstable ($R^2 = 0.38$) and near neutral ($R^2 = 0.55$) conditions.

The poor performance of the LNF theory to estimate NEE above the forest canopy in our study is in agreement with the results reported by Siqueira et al. (2000), who applied the LNF theory to study CO_2 exchange at the Duke Forest in North Carolina. They also evaluated the impact of atmospheric stability conditions on LNF CO_2 fluxes. They

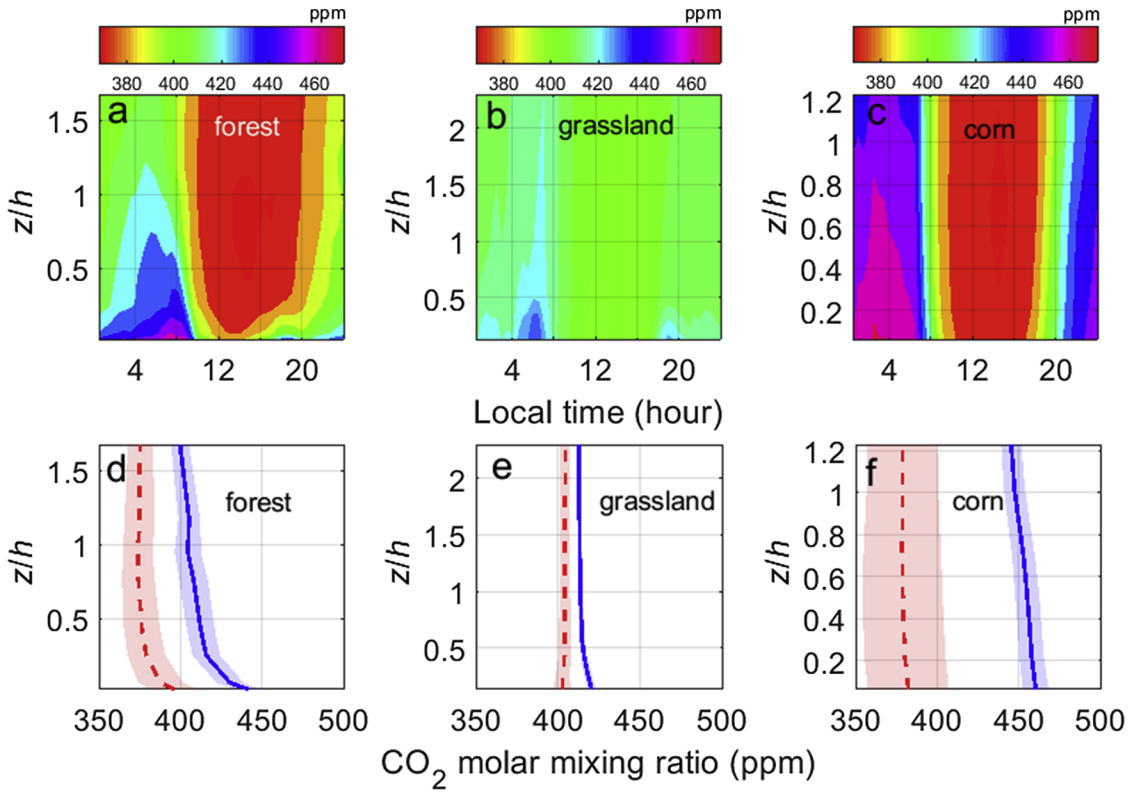

Fig. 2. a, b and c) diel ensemble CO_2 mixing ratio for forest, grassland and corn ecosystems, and d, e and f) mean vertical profiles of CO_2 mixing ratio during daytime (10:00–15:00 h, red dashed lines) and night-time (22:00–3:00 h, blue solid lines). The shaded areas in the bottom panels represent the standard deviation (σ) of CO_2 mixing ratio. (For interpretation of the references to colour in this figure legend, the reader is referred to the web version of this article).

found that LNF performed best for near neutral stability conditions ($R^2 = 0.25$), followed by the unstable atmospheric condition ($R^2 = 0.23$) and stable atmospheric conditions ($R^2 \approx 0$).

Leuning et al. (2000) found that the LNF performance to estimate daytime NEE in a rice canopy was better when $u_* > 0.1\ \mathrm{m\,s^{-1}}$ and under a near neutral stability condition. They also observed that NEE was overestimated by the LNF theory at night, which they attributed to the lack of atmospheric stability corrections to their σ_w and T_L profiles.

Santos et al. (2011) applied an analytical Lagrangian dispersion analysis, proposed by Warland and Thurtell (2000), to infer CO_2 and energy fluxes for a corn canopy. They also applied the atmospheric stability corrections on σ_w and T_L profiles and found the best correlation between measured and modelled NEE for unstable atmospheric conditions and the poorest correlation under stable conditions.

The atmospheric stability corrections used in this manuscript do not account for variations in the local stability regime within plant

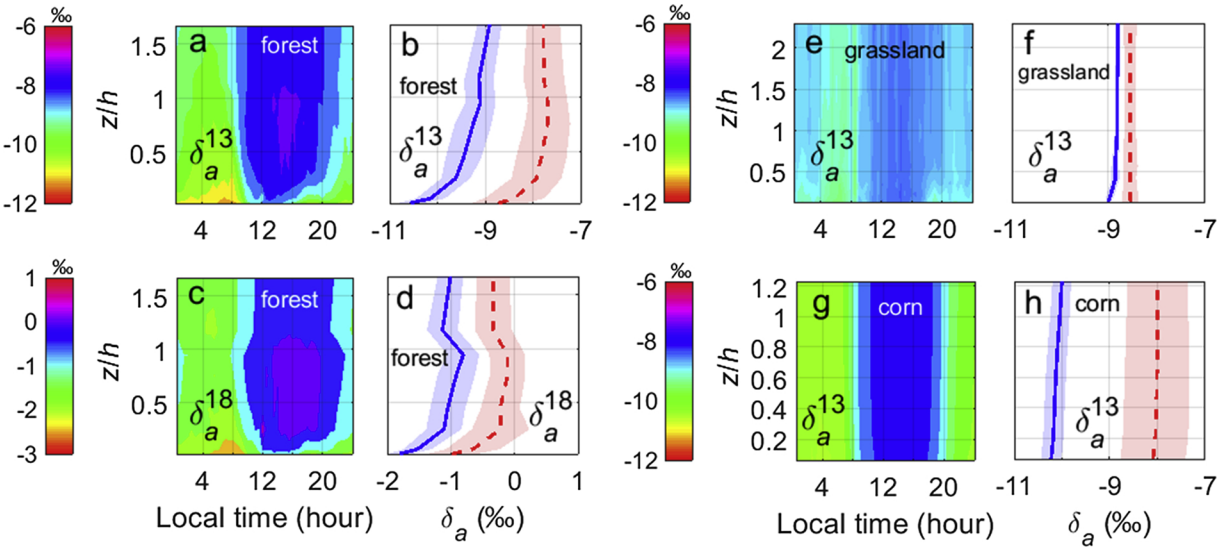

Fig. 3. a, c e and g) ensemble averages of CO_2 isotope compositions of the ambient air (δ_a^{13} and δ_a^{18}) measured within and above forest, grassland and corn canopies; and b, d, f and h) averaged daytime (10:00–15:00 h, red dashed lines) and night-time (22:00–3:00 h, blue solid lines) vertical profiles of δ_a^{13} and δ_a^{18} (for forest) for the same canopies. The shaded areas represent the standard deviation (σ) of δ_a^{13} or δ_a^{18}. (For interpretation of the references to colour in this figure legend, the reader is referred to the web version of this article).

Table 3
Linear regression coefficients for the relationship between net ecosystem CO_2 exchange (NEE) obtained using the eddy covariance method and the LNF theory for different friction velocity screening thresholds.

Ecosystem	u_* (m s^{-1})	n	R^2	Slope	Intercept	d_r
Forest	> 0.1	617	0.03	0.47*	12.8*	0.93
	> 0.2	465	0.09	0.56*	12.5*	0.94
	> 0.3	345	0.18	0.60*	12.1*	0.95
	> 0.4	240	0.35	0.81*	13.6*	0.96
Grassland	> 0.1	564	0.84	0.80*	−0.16*	0.99
	> 0.2	412	0.89	0.84*	−0.22*	0.99
	> 0.3	299	0.91	0.85*	−0.27*	0.99
	> 0.4	179	0.88	0.81*	−0.22*	0.99
Corn	> 0.1	1190	0.45	0.58*	2.04*	0.79
	> 0.2	865	0.48	0.67*	3.11*	0.80
	> 0.3	545	0.57	0.73*	3.84*	0.82
	> 0.4	267	0.72	0.83*	5.21*	0.83

*significant by a t-test at a 5% probability level.

Table 4
Statistical coefficients of the relationship between net ecosystem CO_2 exchange (NEE) obtained using the eddy covariance method and the LNF theory under $u_* > 0.1$ m s^{-1} for different atmospheric stability conditions: unstable ($h/L < -0.01$), neutral ($-0.01 \leq h/L < 0.01$) and stable ($h/L \geq 0.01$) where h/L is the ratio between canopy height and the Obukhov length.

Ecosystem	Stability	NEE				
		n	R^2	Slope	Intercept	d_r
Forest	Unstable	250	0.21	1.92*	43.0*	0.91
	Neutral	25	0.43	1.05*	10.1*	0.97
	Stable	356	0.35	0.97*	2.80*	0.96
Grassland	Unstable	183	0.87	0.81*	−0.35*	0.99
	Neutral	136	0.61	0.72*	−0.03n.s	0.98
	Stable	245	0.20	0.73*	0.45*	0.99
Corn	Unstable	623	0.38	0.76*	4.97*	0.77
	Neutral	204	0.55	0.65*	2.10*	0.79
	Stable	363	0.12	0.42*	1.77*	0.42

canopies. Nevertheless, the stability regime within the canopy can be quite different than the one above the canopy where the wind velocity was measured in this study (Cava et al., 2006). Neglecting the local nature of stability regimes within plant canopies is expected to be quite problematic within dense canopies, such as the forest in this study. In dense canopies, the local temperature variance profile is more complex than inside short canopies with more vigorous turbulent mixing. Consequently, local thermal stratification could alter the relationship between scalar fluxes and mean gradients leading errors in LNF estimates (Cava et al., 2006; Juang et al., 2006).

Therefore, the poor performance of the LNF theory above the forest canopy, when compared to EC NEE measurements, could be related to some degree to the effects of the decoupling between within and above-canopy air flows (Haverd et al., 2009) and local thermal stratification (Cava et al., 2006). Similar to other canopy multilayer models, the LNF assumes that the turbulent transport occurs under steady state conditions, so changes in mass or energy storage within the canopy volume affect the LNF performance.

Katul et al. (1995) used Monin and Obukhov (1954) variance similarity functions to estimate momentum, latent and heat fluxes above a forest canopy. These flux estimates were compared with EC measurements. They reported disagreements between measurements and estimates of latent heat flux which they attributed to water vapour source heterogeneity within the forest canopy. Following Katul et al. (1995), we used the sensible heat flux (H), estimated using the flux-variance relation (FV), as an indicator of the thermal source inhomogeneity within the canopies at the three sites. The FV sensible heat flux is given by:

$$H = \rho c_p \left(\frac{\sigma_T}{C_1}\right)^{\frac{3}{2}} \left(\frac{kgz}{T_a}\right)^{\frac{1}{2}} \quad (11)$$

where ρ and cp are the mean air density (kg m^{-3}) and the specific heat capacity of dry air at constant pressure (= 1005 J kg^{-1} K^{-1}), respectively. $C1$ (= 0.95) is the similarity constant, k (= 0.4) is von Karman's constant, g is the gravitational acceleration (m s^{-2}), σ_T is the standard deviation of sensible heat flux and T_a is the absolute air temperature (K).

We compared the estimated H using Eq. (11) with measurements of H obtained using the EC method. For the forest canopy, the linear relationship between sensible heat fluxes measured using the EC approach and estimated from Eq. (11) had an R^2 of 0.55 and d_r of 0.68. Higher correlation and agreement for the same relationship were found for the grassland canopy (R^2 = 0.72 and d_r = 0.67). For the corn canopy, we observed the strongest correlation and agreement between measured and modelled H, with an R^2 of 0.84 and d_r of 0.76. These results indicate that the canopy heat heterogeneity is higher in the forest than grassland and corn canopies (Cava et al., 2006; Katul et al., 1995). This leads to higher temperature variance for a given sensible heat flux in the forest canopy in relation to the short canopies in this study. This indication of thermal source heterogeneity in the forest canopy could explain, in part, the poor performance of LNF for that canopy.

We also calculated the change in CO_2 storage flux (hereafter CO_2 storage), which was used as an indicator of the degree of flow decoupling between with and above-canopy air flows. The CO_2 storage was calculated following Aubinet et al. (2001) and Papale et al. (2006), as follows:

$$CO_2 \text{ storage} = \frac{P}{R\,T} \int_0^{z_h} \frac{\partial [CO_2](z)}{\partial t} \partial z \quad (12)$$

where P is the atmospheric pressure (Pa), R is the molar gas constant (J mol^{-1} K^{-1}), T is the air temperature (K), [CO_2] is the CO_2 mixing ratio (μmol mol^{-1}), measured at a given height z (m) along a vertical profile with height z_h, and t is time (s). Half-hourly profiles of CO_2 mixing ratio were used in this study to estimate CO_2 storage.

The ensemble-averaged CO_2 storage values calculated from [CO_2] profiles for the different canopies are shown in Fig. 4a. The forest canopy showed the largest depletion rate of stored CO_2 in comparison to the other canopies. The forest depletion rate peak was observed at about 9:00 h and by 15:00 h the canopy air was usually completely well mixed with the air aloft and CO_2 storage approached zero. This diel pattern is in agreement with the results reported by Iwata et al. (2005) who estimated the CO_2 storage in an Amazonian rainforest. The corn canopy showed a much lower depletion rate peak due to the smaller canopy air volume in comparison to the forest. The corn depletion rate peak occurred at about 7:00 h and about 11:00 h the canopy was already well mixed with the atmospheric flow. The grassland canopy showed a negligible change in CO_2 storage throughout the day.

To evaluate the magnitude of the storage term with respect to NEE, we calculated the ratio between CO_2 storage and absolute values of NEE measured by the EC system, following Iwata et al. (2005). The storage/NEE values for the forest canopy were larger than for grassland or corn even under vigorous above canopy turbulence ($u_* > 0.4$ m s^{-1}) (Fig. 4b). These results suggest that atmospheric layers above and within the forest canopy may be fully or partly decoupled leading to large changes in CO_2 storage within the canopy (Haverd et al., 2009; Van Gorsel et al., 2011). This could explain the low correlation between EC and LNF estimates for the forest canopy and a better performance of LNF for the corn and grassland canopies. These results are supported by Göckede et al. (2007)'s findings who used a wavelet tool to characterize several typical states of coupling and decoupling between within-canopy airspace flow and above-canopy flow. They concluded that the flow decoupling is likely to occur in tall canopies with moderate

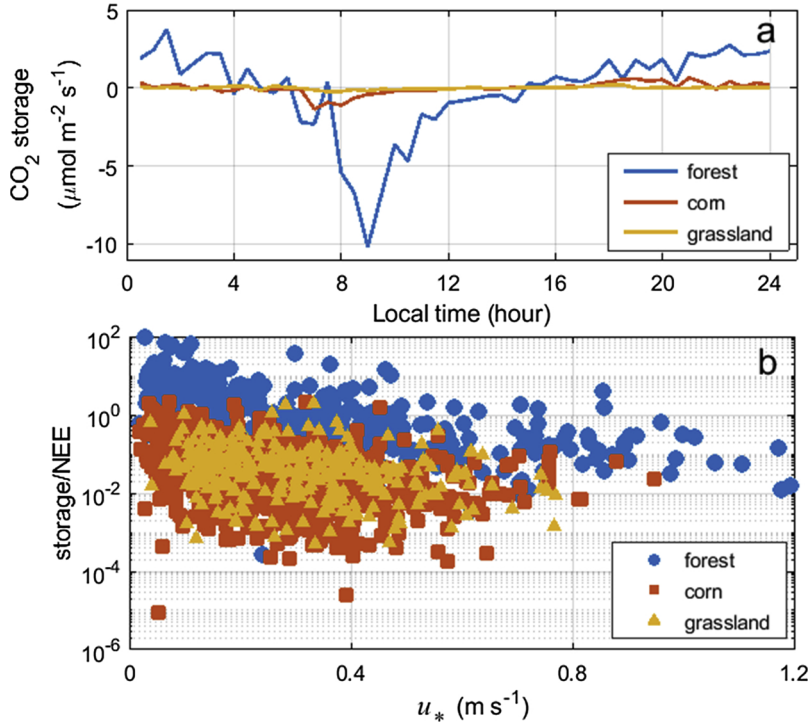

Fig. 4. a) ensemble-averaged CO_2 storage flux estimated for forest, corn and grassland canopies; and b) relationship between the friction velocity (u_*) and the ratio between CO_2 storage and the net CO_2 ecosystem exchange (storage/NEE) for corn, grassland and forest canopies.

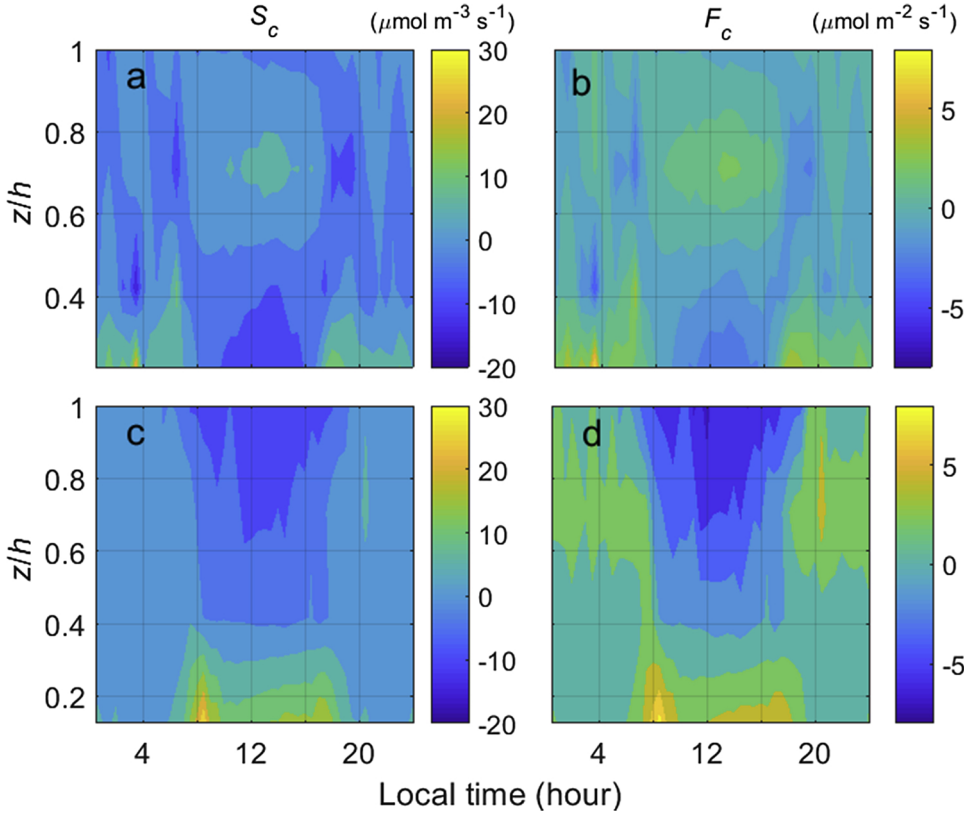

Fig. 5. a and c) spatial and temporal variations of ensemble averaged CO_2 source strength (S_c, μmol m^{-3} s^{-1}), and b and d) CO_2 fluxes (F_c, μmol m^{-2} s^{-1}) estimated using the LNF theory for grassland (a and b) and corn (c and d) canopies.

density, and also suggested that improvements in turbulence statistics considering the decoupling effects could minimize errors in Lagrangian stochastic model estimates.

The ensemble-averaged profiles of CO_2 source strengths (S_c) and CO_2 fluxes (F_c) modelled using the LNF are shown in Fig. 5. We only show S_c estimates for the grassland and corn canopies since the LNF performance to estimate NEE for the forest, and consequently F_c and S_c, was affected by the flow decoupling as discussed previously. We observed a distinct diel variation of S_c for both corn and grassland canopies (Fig. 5a and c), with lower S_c values during daytime than during night-time periods. Corn canopy showed a large CO_2 sink (on average of 13.0 μmol m^{-3} s^{-1}) in the upper layers (z/h > 0.6) and a large CO_2 source (on average of −11.0 μmol m^{-3} s^{-1}) in the bottom layers(z/h < 0.4) during the daytime (Fig. 5c). At night, the corn canopy had a more homogeneous S_c profile, with an average S_c of 2.7 μmol m^{-3} s^{-1} throughout the canopy. The CO_2 flux values also showed a diel trend for both ecosystems (Fig. 5b and d). For the corn canopy (Fig. 5d), a maximum assimilation of −7.0 μmol m^{-2} s^{-1} was observed at midday for top canopy layer (z/h > 0.8). The bottom layers, on the other hand, showed a predominance of respiratory fluxes. A maximum release of 8.9 μmol m^{-2} s^{-1} was observed between 6:30 and 8:30 h at z/h < 0.4 due to a build-up of respiratory fluxes overnight, which extended over all canopy layers during the referred period. For the grassland (Fig. 5b), most assimilation occurred at z/h < 0.6 with a maximum value of −4.2 μmol m^{-2} s^{-1} at 14:00 h and a maximum release of 7.5 μmol m^{-2} s^{-1} observed at bottom layers around 4:00 h. The low assimilation observed for the grassland is related to a reduction in the photosynthetic rates due to the end of growing season. These results suggest that the LNF theory was able to capture the expected spatial and temporal patterns of CO_2 source/sink and CO_2 fluxes for corn and grassland canopies.

The S_c spatial and temporal variability in this study is consistent with the results reported by Hsieh et al. (2003) who proposed the use of a two-dimensional Lagrangian stochastic dispersion model to compute source/sink spatial-temporal variations within a forest canopy. Our results are also in agreement with CO_2 source/sink and flux profiles reported by Leuning et al. (2000) for a rice canopy. They found F_c to be always positive in the lower layers, which agrees with our F_c predictions for the corn canopy. Most studies to date have used the LNF theory to examine scalar exchange in forests, but our results indicate that the LNF theory could be a valuable tool to study scalar exchange in short canopies in which within-canopy EC measurements are not possible with the currently available EC instrumentation.

3.3. Comparison between IFR and LNF isotope compositions of CO_2 fluxes

To investigate the performance of the LNF theory to study isotope exchange in different plant canopies, we compared the LNF estimates of isotope compositions of NEE (δ_N) with the ones provided by the IFR approach (Eq. 10). Previous studies have shown that the magnitude of CO_2 concentration gradients have great impact on IFR estimate uncertainties (Griffis et al., 2005a; Santos et al., 2012). The LNF performance is also expected to be dependent on the accuracy of scalar concentration gradients. In this study, the influence of [CO_2] gradient magnitude on IFR and LNF δ_N estimates was evaluated by calculating the moving coefficient of variation (CV) of δ_N. To do that, δ_N values were sorted based on the ascending order of magnitude of [CO_2] gradients measured by the two highest air intakes. The δ_N CV was then calculated for both methods using the moving standard deviation and moving averages of δ_N for a window size corresponding to four data points.

Fig. 6 shows the relationship between absolute gradients of [CO_2], measured using the two intakes above the canopies, and the CV of δ_N estimated by IFR and LNF approaches. Both methods showed large uncertainties with the IFR δ_N estimates having a larger CV for a given [CO_2] gradient when compared to the LNF estimates. On average, the CV values decreased to less than 100% when [CO_2] gradients exceeded 0.4 ppm m^{-1} for LNF and 0.9 ppm m^{-1} for IFR (Fig. 6a, b and d). However, for the grassland canopy, both methods showed similar δ_N uncertainties, with CV values above 100% for basically all ranges of [CO_2] gradients for both methods (Fig. 6c). Larger gradients of [CO_2] were usually observed for the corn canopy in comparison to the [CO_2] gradients for the other ecosystems (Fig. 6d). These gradients above the corn canopy were likely a result of the placement of the two intakes in a region with strong [CO_2] gradients above the corn canopy (i.e. relatively closer to canopy height) as well as to larger CO_2 fluxes during the growing season when compared to grassland, where CO_2 fluxes were usually smaller near the end of the growing season (Section 3.1).

Previous studies reported large uncertainties in IFR δ_N estimates for small isotopologues concentration gradients, frequently observed just above plant canopies, due to small signal to noise ratio of the concentration data (Griffis et al., 2005a; Santos et al., 2011; Zhang et al., 2006). Our results confirm that δ_N estimate uncertainties are highly dependent on the signal to noise ratio of isotope measurements and that the LNF theory could reduce some of the δ_N uncertainties. Based on the averages of CV, considering all sites, the CV for LNF δ_N estimates was 74% lower than the CV for IFR predictions.

We established an arbitrary screening criterion based on the CV to exclude IFR and LNF δ_N values with large uncertainties. For the CV screening, the δ_N values associated with a CV larger than 70% were excluded from our analyses. The utilization of a CV criterion of 70% was necessary due to the data availability and higher variability of δ_N values, mainly for the grassland. In addition to the CV filter, the LNF and IFR δ_N^{13} estimates smaller than -40‰ and larger than 0‰ were excluded from our analyses. For LNF and IFR δ_N^{18} estimates for the forest, the values excluded were smaller than -40‰ and larger than 40‰.

The IFR and LNF δ_N comparisons are shown in Table 5. In general, the IFR and LNF δ_N estimates showed poor to moderate correlation (R^2 ranging 0.11 to 0.41) and good agreement (d_r ranging from 0.73 to 0.98). We hypothesize that uncertainties in CO_2 isotopologue concentration measurements above the canopies affected the performance of the IFR method. An alternative to increase the signal to noise ratio of the CO_2 isotopologue gradient measurements could be to increase the distance between air intake, and thus the gradients of scalar concentration. In this study, increasing the spacing between air intakes would require the use of air intakes just below the canopy.

The use of in-canopy data in IFR calculations could violate some of the K-theory assumptions due to the proximity of scalar sources and the length scale of turbulence within canopies, leading under some circumstance to counter-gradient fluxes (Corrsin, 1975). To investigate the effect of using in-canopy data on IFR estimates, we calculated δ_N using IFR and concentration data obtained using the highest air intake and the first air intake immediately below the top of the canopies at z/h of 0.94, 0.99 and 0.94 for the forest, grassland and corn canopies, respectively (Table 5). The use of data for larger intake spacing resulted in better correlation (R^2 ranging from 0.57 to 0.68) and agreement (d_r ranging from 0.93 to 0.99) for the relationship between δ_N values estimated using IFR and LNF for the grassland and corn canopies when concentration data for larger intake separation were used in the IFR calculations (Table 5). However, for the forest canopy the use of in-canopy data did not improve the relationships between IFR and LNF δ_N estimates, which could be an indication of K-theory failure for that canopy. Using model simulations, Raupach (1987) demonstrated that counter gradient fluxes resulting from near-field effects can be expected to occur just below a strong scalar source within the canopy. It is possible that due to the forest canopy structure near-field effects were stronger than just below the canopy when compared to the grassland and corn canopies. Furthermore, the IFR approach (Eq. 9) is based on the flux-gradient relation which may be problematic under the complex air flow of the roughness sublayer, especially for forest canopies (Denmead and Bradley, 1987). In forest canopies, the scalar roughness

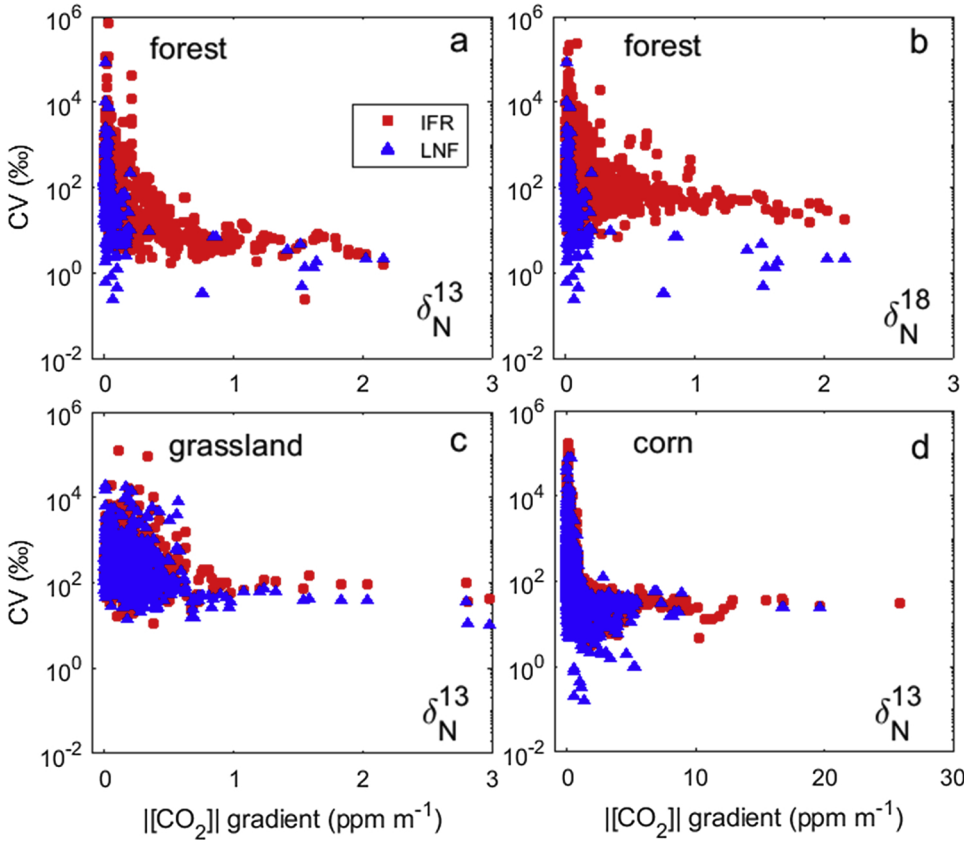

Fig. 6. Relationship between the moving coefficient of variation (CV) of isotope signatures of net CO_2 ecosystem exchange (δ_N^{13} and δ_N^{18}) and the absolute CO_2 mixing ratio vertical gradient. δ_N^{13} and δ_N^{18} were estimated by the IFR method (red squares) and the LNF theory (blue triangles) for different plant canopies. The CV was calculated using moving averages and standard deviations of δ_N^{13} and δ_N^{18} for a window of 4 data points. (For interpretation of the references to colour in this figure legend, the reader is referred to the web version of this article).

Table 5
Statistical coefficients of the relationship between isotope signatures of net ecosystem CO_2 exchange (δ_N) provided by IFR method and predicted from LNF theory.

Ecosystem	δ_N	z_1/h m	n	R^2	Slope	Intercept	d_r
Forest	δ_N^{13}	1.17	125	0.14	0.21[a]	−20.01[a]	0.93
		0.94[b]	216	0.01	−0.02[n.s.]	−25.03[a]	0.98
	δ_N^{18}	1.17	43	0.11	0.43[a]	−5.80[n.s.]	0.96
		0.94[b]	185	0.12	0.08[a]	−7.49[*]	0.95
Grassland	δ_N^{13}	1.53	12	0.18	0.52[n.s.]	−13.99[n.s.]	0.73
		0.99[+]	36	0.68	0.78[a]	−4.37[n.s.]	0.99
Corn	δ_N^{13}	1.15	470	0.41	0.49[a]	−8.40[a]	0.86
		0.94[b]	594	0.57	0.55[a]	−7.53[a]	0.93

n.s., not significant by a *t*-test at a 5% probability level.
[a] significant by a *t*-test at 5% probability level.
[b] z_1 slightly inside the canopy.

sublayer is much 'thicker' than its momentum counterpart (Raupach and Thorn, 1981). Thus, local mean concentration gradients alone could explain the local fluxes in the grassland and corn canopies, but not likely in the forest.

Our results show that both IFR and LNF methods can capture seasonal variation in δ_N^{13} (Fig. 7). The seasonal averages of δ_N^{13} provided by IFR and LNF for the corn canopy were -20.6 and -18.5‰, respectively. The temporal variation of δ_N^{13} showed a downward trend toward the end of the growing season. This seasonal variation in δ_N^{13} was likely due to a larger contribution of C_3 residue in the soil organic matter to the ecosystem respiration in comparison to flux contributions from corn plants

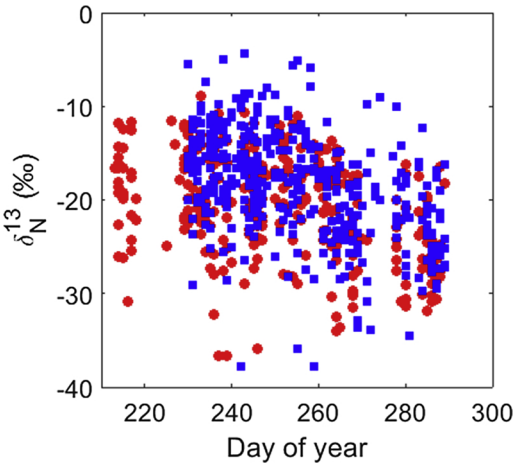

Fig. 7. Seasonal variation in the isotope composition of net ecosystem $^{13}CO_2$ exchange (δ_N^{13}) estimated using the IFR (red circles) and LNF theory (blue squares) for the corn canopy. (For interpretation of the references to colour in this figure legend, the reader is referred to the web version of this article).

that were reaching senescence. A similar trend was observed in previous studies carried out in corn/soybean rotations (Griffis et al., 2008, 2005a).

Fig. 8 shows the half-hourly averaged vertical distribution of the isotope composition of CO_2 flux (δ_F) estimated by LNF for different canopies. Unfortunately, we were unable to plot the δ_F vertical distribution for the grassland canopy due to the low data availability after data screening procedures (Section 3.3). Larger variability in δ_F were

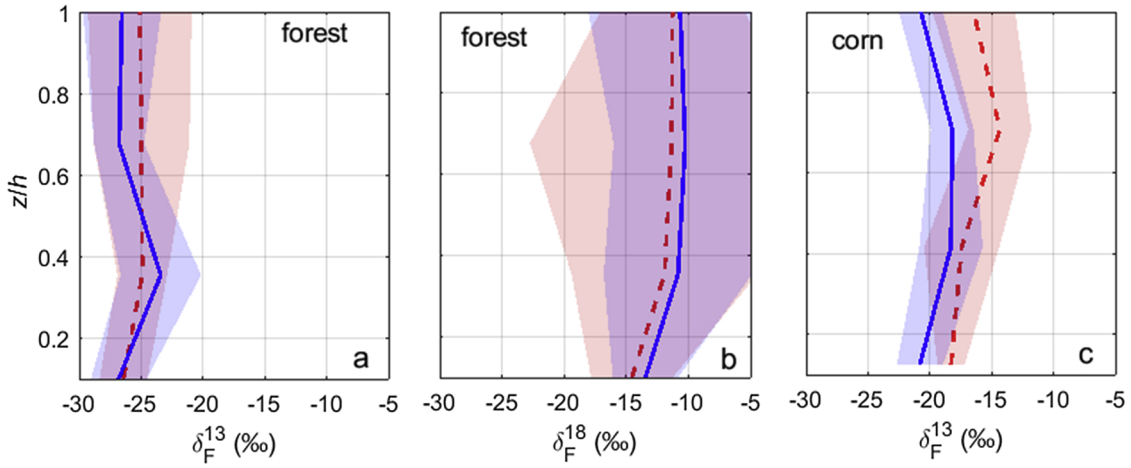

Fig. 8. Half-hourly averaged vertical distribution of isotope composition of CO_2 flux (δ_F^{13} and δ_F^{18}) estimated using the LNF theory for different plant canopies during daytime (red dashed lines) and nighttime (blue solid lines) periods. The shaded areas represent the standard deviation (σ) of δ_F^{13} or δ_F^{18}. (For interpretation of the references to colour in this figure legend, the reader is referred to the web version of this article).

found for the forest canopy (Fig. 8a and b) in comparison to the δ_F variability observed for the corn canopy (Fig. 8c). For the corn canopy, where the mean standard deviation (σ) was lower than for the forest, the average LNF δ_F^{13} (± σ) during the daytime was -17.8‰ (± 2.0‰) for the source layer below z/h < 0.4 and -15.4‰ (± 2.9) for other source layers. At night a similar pattern was observed, i.e. more depleted LNF δ_F^{13} for the source layers near the ground with a lower value of -20.8‰ (± 1.8) than for higher source layers of −19.0‰ (± 1.9). The range of δ_F^{13} and δ_F^{18} values provided by the LNF in these vertical distributions are in agreement with those found in previous studies with C_3 and C_4 ecosystems (Griffis et al., 2008, 2005a; Santos et al., 2014, 2012). The large variability in δ_F^{18} could be a result of the high temporal dynamics of the $C^{18}OO$ isopologue at the forest ecosystem, which agrees with the data provided by Santos et al. (2014) for that ecosystem.

3.4. Estimating the ^{13}C isoforcing

To quantify the effect of isotope biosphere-atmosphere exchange on the δ_a^{13} budget, we calculated the ecosystem-scale ^{13}C isoforcing (I_F) following Griffis et al. (2008) and Lee et al. (2009).

$$I_F = \frac{NEE}{c_a}(\delta_N^{13} - \delta_a^{13}) \quad (13)$$

where, NEE is the net CO_2 ecosystem exchange (μmol $m^{-2} s^{-1}$), c_a is the half-hour CO_2 concentration (μmol m^{-3}), and δ_N^{13} is the ^{13}C composition of ambient air (‰).

We calculated I_F using two different approaches by combining EC measurements of NEE: 1) with flux ratios (δ_N^{13}) estimated by the IFR method and 2) δ_N^{13} estimated using the LNF theory. Following Sturm et al. (2012), we also calculated a hypothetical isoforcing for both IFR and LNF methods. The hypothetical isoforcing were calculated using constants of δ_N^{13} of -20.6 and -18.5‰, which correspond to the average δ_N^{13} estimated by IFR and LNF methods, respectively. Unfortunately, we were unable to perform the same calculation for forest and grassland canopies due to the low data availability after data screening procedures (Section 3.3).

The ensemble-averaged diel of δ_N^{13} calculated by IFR and LNF approaches for the corn canopy is shown in Fig. 9. Large fluctuations were observed in IFR δ_N^{13} estimates mainly between 6:00 and 18:00 h (Fig. 9a). This large variability in δ_N^{13} is a result of small concentration gradients of [CO_2] observed during daytime periods under turbulent conditions (see Section 3.1). The LNF estimates of δ_N^{13} were less variable than IFR estimates (Fig. 9b).

The diurnal pattern of I_F was mainly driven by the NEE diel variation. The large variability in IFR I_F estimates during daytime periods were a result of the large uncertainties in IFR estimates (Fig. 9c). The LNF I_F estimate uncertainties were lower than the IFR estimates (Fig. 9d). Estimated LNF I_F show a small difference between the hypothetical isoforcing and LNF I_F of 0.003 m s^{-1} ‰ (± 0.003 m s^{-1} ‰) during daytime between 8:00 and 11:00 h. Large difference is observed between 11:30 h and 15:30 of 0.005 m s^{-1} ‰ (± 0.002 m s^{-1} ‰), which the maximum difference was found at 12:00 with a value of 0.009 m s^{-1} ‰. This may be an indication that δ_N^{13} contributed to some degree to the isoforcing's diurnal variation, as supported by the LNF δ_N^{13} values that showed a small diurnal variation with δ_N^{13} values ranging from −15.8‰ to −20.3‰ (Fig. 9b). This suggests a small isotopic disequilibrium for the corn ecosystem. The large inherent noises of the IFR method (Fig. 9a) limited the use of IFR I_F for constraining isotope budgets (Sturm et al., 2012)

4. Conclusions

In this study, we evaluated the use of the localized near-field theory (LNF) to study $^{13}CO_2$ and $C^{18}OO$ isotope exchange in different plant canopies. The LNF estimates of NEE were highly sensitive to the below and above canopy flow decoupling. The large depletion peak of CO_2 storage associated with strong flow decoupling in the forest canopy was shown to affect the NEE estimates from LNF, which showed the lowest correlation (R^2 = 0.35) with NEE measured using the EC technique. For the corn and grassland, where the depletion peak of CO_2 storage was found to be very small or negligible, the model performed better than forest with R^2 of 0.72 and 0.88, respectively. These results suggest that the LNF theory may provide better estimates for short canopies, in which there is lower CO_2 storage within canopy airspace in comparison to forest canopies. This could be a great advantage of LNF to study scalar transport within short canopies since the EC instrumentation is too bulky to be used to measure fluxes within short canopies.

The CV for LNF δ_N estimates was 74% lower than the CV for IFR predictions and, therefore the LNF theory can reduce some of the IFR δ_N uncertainties. The period of measurement near the end of growing season for the grassland contributed to a smaller spatial variation of [CO_2] than forest and corn, thus leading to an even smaller precision of the methods in this specific case. On average, the CV values decreased to less than 100% when [CO_2] gradients exceeded 0.4 ppm m^{-1} for LNF and 0.9 ppm m^{-1} for IFR. However, for the grassland canopy, both methods showed similar δ_N uncertainties, showing high relative variability with values of CV larger than 100% for practically all [CO_2] gradient ranges. The correlation (R^2) between δ_N IFR and δ_N LNF estimates for grassland and corn canopies increased, on average, from 0.29

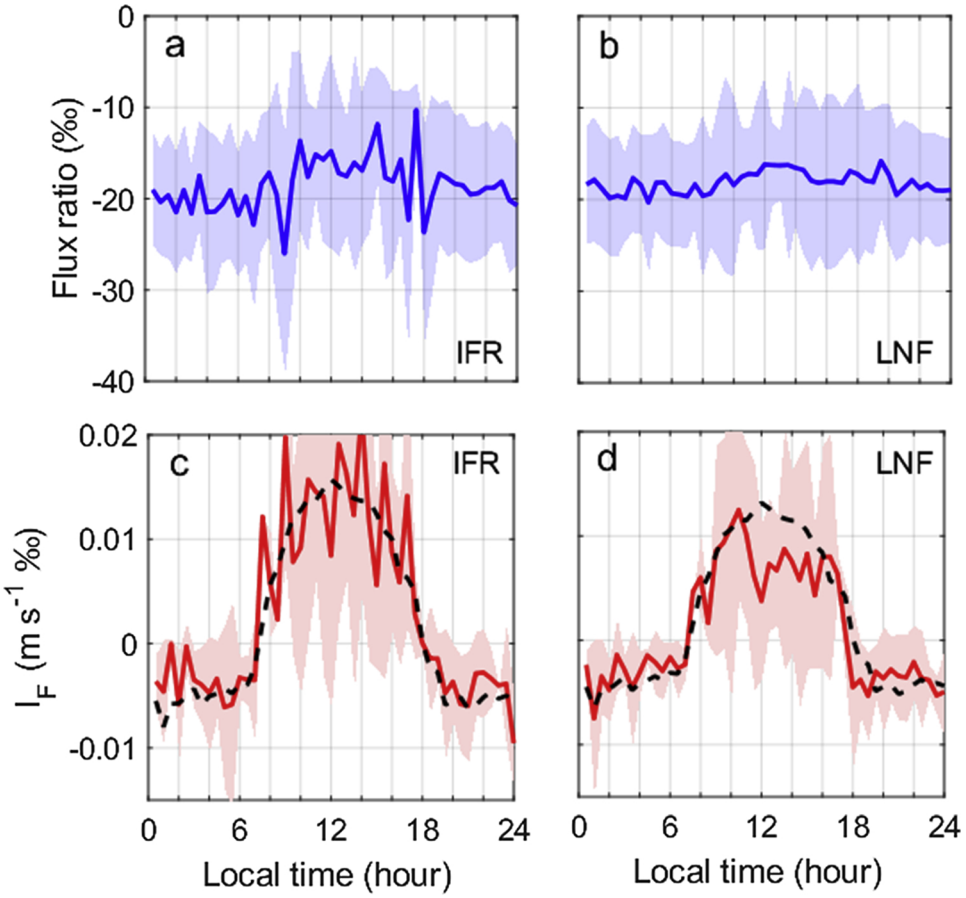

Fig. 9. a and b) ensemble average of $^{13}CO_2$ compositions of NEE (δ_N^{13}) estimated using the IFR method and LNF theory for the corn canopy; and c and d) mean diurnal ^{13}C isoforcing (I_F) calculated combining eddy covariance NEE measurements with: δ_N^{13} provided by IFR method and δ_N^{13} predicted by the LNF theory. The dashed lines represent the calculated hypothetical isoforcing with a constant δ_N^{13} of −20.6 and −18.5‰ for IFR and LNF, respectively. The shaded areas represent the standard deviation (σ) of flux ratio or I_F.

to 0.62 and the agreement approached one (d_r increased, on average, from 0.79 to 0.96) when IFR was calculated using one air intake of measurement slightly inside the canopy.

Our study shows the first attempt to combine LNF predictions with several months of near-continuous measurements of stable isotopes of CO_2 in different vegetation canopies. These results indicate that LNF is potentially a useful tool to provide new insights to study CO_2 exchange processes within well-mixed short canopies, where the flux measurements using traditional micrometeorological techniques are even more challenging. In addition, LNF also can be useful for inferring isotope exchange within plant canopies, which allows the separation of the isotope exchange between soil and plant components.

Acknowledgements

Funding for this research was provided by the Natural Science and Engineering Research Council and National Science Foundation (grant number EPS-0903806). Contribution no. 19-206-J from the Kansas Agricultural Experiment Station. The first author stipend was funded by Coordination for the Improvement of Higher Education Personnel (CAPES). We would like to thank the late scientists Mike Raupach and Tom Denmead for suppling us with the LNF source code during the initial stages of this research project. We are also thankful to Dean Loutitt for his assistance of the field work. We would like to thank the reviewers for the insightful suggestions to improve this manuscript.

References

Aubinet, M., Chermanne, B., Vandenhaute, M., Longdoz, B., Yernaux, M., Laitat, E., 2001. Long term carbon dioxide exchange above a mixed forest in the Belgian Ardennes. Agric. For. Meteorol. 108, 293–315. https://doi.org/10.1016/S0168-1923(01)00244-1.

Baldocchi, D.D., 2003. Assessing the eddy covariance technique for evaluating carbon dioxide exchange rates of ecosystems: past, present and future. Glob. Chang. Biol. 479–492. https://doi.org/10.1046/j.1365-2486.2003.00629.x.

Brown, S.E., Wagner-Riddle, C., 2017. Assessment of random errors in multi-plot nitrous oxide flux gradient measurements. Agric. For. Meteorol. 242, 10–20. https://doi.org/10.1016/j.agrformet.2017.04.005.

Buchmann, N., Ehleringer, J.R., 1998. CO_2 concentration profiles, and carbon and oxygen isotopes in C_3 and C_4 crop canopies. Agric. For. Meteorol. 89, 45–58. https://doi.org/10.1016/S0168-1923(97)00059-2.

Buchmann, N., Kao, W.Y., Ehleringer, J.R., 1996. Carbon dioxide concentrations within forest canopies - variation with time, stand structure, and vegetation type. Glob. Chang. Biol. 2, 421–432. https://doi.org/10.1111/j.1365-2486.1996.tb00092.x.

Cava, D., Katul, G.G., Scrimieri, A., Poggi, D., Cescatti, A., Giostra, U., 2006. Buoyancy and the sensible heat flux budget within dense canopies. Boundary-Layer Meteorol. 118, 217–240. https://doi.org/10.1007/s10546-005-4736-1.

Corrsin, S., 1975. Limitations of gradient transport models in random walks and in turbulence. Adv. Geophys. 18, 25–60. https://doi.org/10.1016/S0065-2687(08)60451-3.

Denmead, O.T., Bradley, E.F., 1987. On scalar transport in plant canopies. Irrig. Sci. 8, 131–149. https://doi.org/10.1007/BF00259477.

Farquhar, G.D., Ehleringer, J.R., Hubick, K.T., 1989. Carbon isotope discrimination and photosynthesis. Plant Physiol. Plant Mol. Biol. 40, 503–537. https://doi.org/10.1146/annurev.pp.40.060189.002443.

Flanagan, L.B., Brooks, J.R., Varney, G.T., Berry, S.C., Ehleringer, J.R., 1996. Carbon isotope discrimination during photosynthesis and the isotope ratio of respired CO_2 in boreal forest ecosystems. Global Biogeochem. Cycles 10, 629–640. https://doi.org/10.1029/96GB02345.

Göckede, M., Thomas, C., Markkanen, T., Mauder, M., Ruppert, J., Foken, T., 2007. Sensitivity of Lagrangian Stochastic footprints to turbulence statistics. Tellus, Ser. B Chem. Phys. Meteorol. 59, 577–586. https://doi.org/10.1111/j.1600-0889.2007.

00275.x.
Griffis, T., Sargent, S., Baker, J., Lee, X., Tanner, B., Greene, J., Swiatek, E., Billmark, K., 2008. Direct measurement of biosphere-atmosphere isotopic CO_2 exchange using the eddy covariance technique. J. Geophys. Res. Atmos. 113, D08304. https://doi.org/10.1029/2007JD009297.
Griffis, T.J., 2013. Tracing the flow of carbon dioxide and water vapor between the biosphere and atmosphere: a review of optical isotope techniques and their application. Agric. For. Meteorol. 174–175, 85–109. https://doi.org/10.1016/j.agrformet.2013.02.009.
Griffis, T.J., Baker, J.M., Sargent, S.D., Tanner, B.D., Zhang, J., 2004. Measuring field-scale isotopic CO_2 fluxes with tunable diode laser absorption spectroscopy and micrometeorological techniques. Agric. For. Meteorol. 124, 15–29. https://doi.org/10.1016/j.agrformet.2004.01.009.
Griffis, T.J., Baker, J.M., Zhang, J., 2005a. Seasonal dynamics and partitioning of isotopic CO_2 exchange in a C_3/C_4 managed ecosystem. Agric. For. Meteorol. 132, 1–19. https://doi.org/10.1016/j.agrformet.2005.06.005.
Griffis, T.J., Lee, X., Baker, J.M., Billmark, K., Schultz, N., Erickson, M., Zhang, X., Fassbinder, J., Xiao, W., Hu, N., 2011. Oxygen isotope composition of evapotranspiration and its relation to C_4 photosynthetic discrimination. J. Geophys. Res. Biogeosciences 116, 1–21. https://doi.org/10.1029/2010JG001514.
Griffis, T.J., Lee, X., Baker, J.M., Sargent, S.D., King, J.Y., 2005b. Feasibility of quantifying ecosystem-atmosphere $C^{18}O^{16}O$ exchange using laser spectroscopy and the flux-gradient method. Agric. For. Meteorol. 135, 44–60. https://doi.org/10.1016/j.agrformet.2005.10.002.
Harper, L., Denmead, O., Sharpe, R., 2000. Identifying sources and sinks of scalars in a corn canopy with inverse Lagrangian dispersion analysis: II. Ammonia. Agric. For. Meteorol. 104, 75–83. https://doi.org/10.1016/S0168-1923(00)00149-0.
Haverd, V., Cuntz, M., Griffith, D., Keitel, C., Tadros, C., Twining, J., 2011. Measured deuterium in water vapour concentration does not improve the constraint on the partitioning of evapotranspiration in a tall forest canopy, as estimated using a soil vegetation atmosphere transfer model. Agric. For. Meteorol. 151, 645–654. https://doi.org/10.1016/j.agrformet.2011.02.005.
Haverd, V., Leuning, R., Griffith, D., van Gorsel, E., Cuntz, M., 2009. The turbulent Lagrangian time scale in forest canopies constrained by fluxes, concentrations and source distributions. Boundary-Layer Meteorol. 130, 209–228. https://doi.org/10.1007/s10546-008-9344-4.
Hsieh, C.-I., Siqueira, M., Katul, G., Chu, C.-R., 2003. Predicting scalar source-sink and flux distributions within a forest canopy using a 2-D Lagrangian stochastic dispersion model. Boundary-Layer Meteorol. 109, 113–138. https://doi.org/10.1023/A:1025461906331.
Iwata, H., Malhi, Y., Von Randow, C., 2005. Gap-filling measurements of carbon dioxide storage in tropical rainforest canopy airspace. Agric. For. Meteorol. 132, 305–314. https://doi.org/10.1016/j.agrformet.2005.08.005.
Juang, J.Y., Katul, G.G., Siqueira, M.B.S., Stoy, P.C., Palmroth, S., McCarthy, H.R., Kim, H.S., Oren, R., 2006. Modeling nighttime ecosystem respiration from measured CO_2 concentration and air temperature profiles using inverse methods. J. Geophys. Res. Atmos. 111, 1–16. https://doi.org/10.1029/2005JD005976.
Katul, G., Albertson, J., 1999. Modeling CO_2 sources, sinks and fluxes within a forest canopy. J. Geophys. Res. Atmos. 104, 6081–6091. https://doi.org/10.1029/1998JD200114.
Katul, G., Goltz, S.M., Hsieh, C.-I., Cheng, Y., Mowry, F., Sigmon, J., 1995. Estimation of surface heat and momentum fluxes using the flux-variance method above uniform and non-uniform terrain. Boundary-Layer Meteorol. 74, 237–260. https://doi.org/10.1007/BF00712120.
Katul, G., Oren, R., Ellsworth, D., Hsieh, C., Phillips, N., 1997. A Lagrangian dispersion model for predicting sources, sinks, and fluxes in a uniform loblolly pine (Pinus taeda L.) stand. J. Geophys. Res. 102, 9309–9321. https://doi.org/10.1029/96JD03785.
Lee, X., Griffis, T.J., Baker, J.M., Billmark, K.A., Kim, K., Welp, L.R., 2009. Canopy-scale kinetic fractionation of atmospheric carbon dioxide and water vapor isotopes. Global Biogeochem. Cycles 23, 1–15. https://doi.org/10.1029/2008GB003331.
Leuning, R., 2000. Estimation of scalar source/sink distributions in plant canopies using Lagrangian dispersion analysis: corrections for atmospheric stability and comparison with a multilayer canopy model. Boundary-Layer Meteorol. 96, 293–314. https://doi.org/10.1023/A:1002449700617.
Leuning, R., Denmead, O.T., Miyata, A., Kim, J., 2000. Source/sink distributions of heat, water vapour, carbon dioxide and methane in a rice canopy estimated using Lagrangian dispersion analysis. Agric. For. Meteorol. 104, 233–249. https://doi.org/10.1016/S0168-1923(00)00158-1.
Monin, A.S., Obukhov, A.M., 1954. Basic laws of turbulent mixing in the surface layer of the atmosphere. Orig. Publ. Tr. Akad. Nauk SSSR Geophiz. Inst 24, 163–187.
Papale, D., Reichstein, M., Aubinet, M., Canfora, E., Bernhofer, C., Kutsch, W., Longdoz, B., Rambal, S., Valentini, R., Vesala, T., Yakir, D., 2006. Towards a standardized processing of net ecosystem exchange measured with eddy covariance technique: algorithms and uncertainty estimation. Biogeosciences 3, 571–583. https://doi.org/10.5194/bg-3-571-2006.
Raupach, M.R., 2001. Inferring biogeochemical sources and sinks from atmospheric concentrations: General considerations and applications in vegetation canopies. Global Biogeochemical Cycles in the Climate System. pp. 41–59. https://doi.org/10.1016/B978-012631260-7/50006-6.
Raupach, M.R., 1989a. Applying Lagrangian fluid mechanics to infer scalar source distributions from concentration profiles in plant canopies. Agric. For. Meteorol. 47, 85–108. https://doi.org/10.1016/0168-1923(89)90089-0.
Raupach, M.R., 1989b. A practical Lagrangian method for relating scalar concentrations to source distributions in vegetation canopies. Q. J. R. Meteorol. Soc. 115, 609–632. https://doi.org/10.1002/qj.49711548710.
Raupach, M.R., 1989c. Stand overstorey processes. Philos. Trans. R. Soc. Lond., B, Biol. Sci. 324, 175–190. https://doi.org/10.1098/rstb.1989.0043.
Raupach, M.R., 1987. A Lagrangian analysis of scalar transfer in vegetation canopies. Q. J. R. Meteorol. Soc. 113, 107–120. https://doi.org/10.1002/qj.49711347507.
Raupach, M.R., Denmead, O.T., Dunin, F.X., 1992. Challenges in linking atmospheric CO_2 concentrations to fluxes at local and regional scales. Aust. J. Bot. 40, 697–716. https://doi.org/10.1071/BT9920697.
Raupach, M.R., Thorn, A.S., 1981. Turbulence in and above plant canopies. Annu. Rev. Fluid Mech. 13, 97–129. https://doi.org/10.1146/annurev.fl.13.010181.000525.
SanClements, M., Metzger, S., Luo, H., Pingintha-Durden, N., Zulueta, R.C., Loescher, H.W., 2014. The National Ecological Observatory Network (NEON): providing free long-term ecological data on a continental scale. iLEAPS Newsletter. Special Issue on Environmental Research Infrastructures 23–26.
Santos, E., Wagner-Riddle, C., Lee, X., Warland, J., Brown, S., Staebler, R., Bartlett, P., Kim, K., 2014. Temporal dynamics of oxygen isotope compositions of soil and canopy CO_2 fluxes in a temperate deciduous forest. J. Geophys. Res. Biogeosciences 996–1013. https://doi.org/10.1002/2013JG002525.Received.
Santos, E., Wagner-Riddle, C., Lee, X., Warland, J., Brown, S., Staebler, R., Bartlett, P., Kim, K., 2012. Use of the isotope flux ratio approach to investigate the $C^{18}O^{16}O$ and $^{13}CO_2$ exchange near the floor of a temperate deciduous forest. Biogeosciences 9, 2385–2399. https://doi.org/10.5194/bg-9-2385-2012.
Santos, E.A., Wagner-Riddle, C., Warland, J.S., Brown, S., 2011. Applying a Lagrangian dispersion analysis to infer carbon dioxide and latent heat fluxes in a corn canopy. Agric. For. Meteorol. 151, 620–632. https://doi.org/10.1016/j.agrformet.2011.01.010.
Siqueira, M., Lai, C.T., Katul, G., 2000. Estimating scalar sources, sinks, and fluxes in a forest canopy using Lagrangian, Eulerian, and hybrid inverse models. J. Geophys. Res. Atmos. 105, 29475–29488. https://doi.org/10.1029/2000JD900543.
Stropes, K.S., 2017. Investigating the Exchange of CO_2 in a Tall-grass Prairie Ecosystem Using Stable Isotopes and Micrometeorological Methods. Kansas State University.
Sturm, P., Eugster, W., Knohl, A., 2012. Eddy covariance measurements of CO_2 isotopologues with a quantum cascade laser absorption spectrometer. Agric. For. Meteorol. 152, 73–82. https://doi.org/10.1016/j.agrformet.2011.09.007.
Styles, J.M., Raupach, M.R., Farquhar, G.D., Kolle, O., Lawton, K.A., Brand, W.A., Werner, R.A., Jordan, A., Schulze, E.-D., Shibistova, O., Lloyd, J., 2002. Soil and canopy CO_2, $^{13}CO_2$, H_2O and sensible heat flux partitions in a forest canopy inferred from concentration measurements. Tellus, Ser. B Chem. Phys. Meteorol. 54, 655–676. https://doi.org/10.3402/tellusb.v54i5.16708.
Taylor, G.I., 1922. Diffusion by continuous movements. Proc. london Math. Soc. 2, 196–212. https://doi.org/10.1112/plms/s2-20.1.196.
Ueyama, M., Takanashi, S., Takahashi, Y., 2014. Inferring methane fluxes at a larch forest using Lagrangian, Eulerian, and hybrid inverse models. J. Geophys. Res. G Biogeosciences 119, 2018–2031. https://doi.org/10.1002/2014JG002716.
Van Gorsel, E., Harman, I.N., Finnigan, J.J., Leuning, R., 2011. Decoupling of air flow above and in plant canopies and gravity waves affect micrometeorological estimates of net scalar exchange. Agric. For. Meteorol. 151, 927–933. https://doi.org/10.1016/j.agrformet.2011.02.012.
Warland, J.S., Thurtell, G.W., 2000. A Lagrangian solution to the relationship between source strength and concentration profile under conditions of local advection. Boundary-Layer Meteorol. 96, 453–471. https://doi.org/10.1007/s10546-006-9098-9.
Wehr, R., Munger, J.W., Nelson, D.D., Mcmanus, J.B., Zahniser, M.S., Wofsy, S.C., Saleska, S.R., 2013. Long-term eddy covariance measurements of the isotopic composition of the ecosystem – atmosphere exchange of CO_2 in a temperate forest. Agric. For. Meteorol. 181, 69–84. https://doi.org/10.1016/j.agrformet.2013.07.002.
Wehr, R., Saleska, S.R., 2015. An improved isotopic method for partitioning net ecosystem – atmosphere CO_2 exchange. Agric. For. Meteorol. 214–215, 515–531. https://doi.org/10.1016/j.agrformet.2015.09.009.
Werner, C., Schnyder, H., Cuntz, M., Keitel, C., Zeeman, M.J., Dawson, T.E., Badeck, F., Brugnoli, E., 2012. Progress and challenges in using stable isotopes to trace plant carbon and water relations across scales. Biogeosciences 9, 3083–3111. https://doi.org/10.5194/bg-9-3083-2012.
Willmott, C.J., Robeson, M., Matsuura, K., 2012. A refined index of model performance. Int. J. Climatol. 32, 2088–2094. https://doi.org/10.1002/joc.2419.
Xiao, J., Chen, J., Davis, K.J., Reichstein, M., 2012. Advances in upscaling of eddy covariance measurements of carbon and water fluxes. J. Geophys. Res. Biogeosciences 117, 0–5. https://doi.org/10.1029/2011JG001889.
Yakir, D., Sternberg, S.L., 2000. The use of stable isotopes to study ecosystem gas exchange. Oecologia 297–311. https://doi.org/10.1007/s004420051016.
Zhang, J., Griffis, T.J., Baker, J.M., 2006. Using continuous stable isotope measurements to partition net ecosystem CO2 exchange. Plant Cell Environ. 29, 483–496. https://doi.org/10.1111/j.1365-3040.2005.01425.x.